Controlled Ordering of Block Copolymer Thin Films by the Addition of Hydrophilic Nanoparticles

Sung Chan Park,[†] Bumjoon J. Kim,[‡,⊥] Craig J. Hawker,[‡,§,#] Edward J. Kramer,[*,‡,§,⊥] Joona Bang,[*,†] and Jeong Sook Ha[*,†]

Department of Chemical and Biological Engineering, Korea University, Seoul 136-701, Republic of Korea; Materials Research Laboratory, University of California, Santa Barbara, California 93106; Department of Materials, University of California, Santa Barbara, California 93106; Department of Chemical Engineering, University of California, Santa Barbara, California 93106; and Department of Chemistry and Biochemistry, University of California, Santa Barbara, California 93106

Received June 28, 2007
Revised Manuscript Received August 6, 2007

Introduction

The spatial arrangement of nanostructures such as inorganic nanoparticles in a host matrix or domains in block copolymer thin films has been extensively studied due to their potential applications in diverse fields ranging from block copolymer lithography to advanced catalysts and solar cells.[1−24] The key issue in all of these systems is to control the orientation and location of either the nanoparticles or polymeric domains. In terms of nanoparticles, Balazs and co-workers have recently suggested that the nanoparticle position can be simply controlled by the ratio d/L, where d is the particle size and L is the size of block copolymer domain.[5−7] When $d/L \geq 0.3$, they predict that the particles are localized around the center of domain due to the chain stretching penalty, while the particles move outward to the interface when d/L becomes smaller. Several experimental approaches have been developed to confirm this prediction,[8−10] and more recent work has examined the effect of chemistry where the surface of nanoparticle is tuned to allow favorable interactions between nanoparticles and block copolymers, which in turn allows their location to be influenced.[11−14]

In addition to controlling the location of the nanoparticles, it would be highly desirable if the nanoparticles could also play an "active" role in the self-assembly process, such as directing the morphology and orientation of microstructures. In this regards, pioneering work has been performed by Emrick and Russell,[15] where incorporation of cadmium selenide nanoparticles into block copolymer thin films can mediate interfacial interactions and control the orientation of microdomains. More recently, Kim showed that stable bicontinuous morphologies with nanoscale dimensions can be fabricated by the addition of "neutral" nanoparticles which are directed to and stabilize the interface between diblock copolymers.[16]

This growing importance of block copolymer orientation is also exemplified and highlighted by the IBM announcement of large-scale manufacturing of devices incorporating air gaps fabricated using PSt-*b*-PMMA block copolymer templates. For block copolymers, the classical approach to control the orientation of PSt-*b*-PMMA systems is to introduce an ultrathin random copolymer neutralization layer in a secondary process.[17−19] This neutralization layer is not required for poly(ethylene oxide) (PEO)-based block copolymer systems where the morphologies and orientation of the thin films are controlled and greatly affected by the relative humidity during a solvent annealing process, though removal of the PEO domain is difficult.[25−28] In this case, it was found that interaction between the water vapor in the atmosphere and the PEO domains leads to lateral ordering of the PEO microdomains, and application of this process to PSt-*b*-PMMA systems did not lead to orientation. In this paper, we demonstrate a novel method to control the orientation of PSt-*b*-PMMA block copolymer thin films using hydrophilic nanoparticles without the need for a neutralization layer, greatly improving the processability of PSt-*b*-PMMA systems. By incorporating "hydrophilic" PEO-coated nanoparticles into poly(styrene-*b*-methyl methacrylate) (PSt-*b*-PMMA) diblock copolymers, the ordering of PSt-*b*-PMMA thin films can be effectively controlled in a manner similar to the PEO-based block copolymer while retaining the degradability of the PMMA domains. In addition, the effect of hydrophilic PEO-coated Au particles on the domain size and its homogeneity of PMMA cylinders within a PS domain is demonstrated while the nanoparticle itself holds promise for introducing secondary functionality such as etch resistance into the films.

Experimental Section

Materials. Poly(styrene-*b*-methyl methacrylate) (PSt-*b*-PMMA) diblock copolymer, showing a cylindrical microstructure, was synthesized via living anionic polymerization. The overall molecular weight, 140 kg/mol, and polydispersity, 1.06, were measured from size exclusion chromatography (SEC), using refractive index and photodiode array detectors (Waters), and the block composition was determined from ^{1}H NMR using a Bruker 200 MHz spectrometer.

PEO-coated gold nanoparticles (Au-PEO) were synthesized as follows: Initially, thiol end-functional PEO (PEO-SH, Polymer Source, $M_n = 2$ kg/mol) and gold precursors ($HAuCl_4$) were dissolved into dry THF and mixed for 15 min under a nitrogen atmosphere.[29] Gold nanoparticles were synthesized by adding a reducing agent, superhydride (1.0 M $Li(C_2H_5)_3BH$ in THF from Sigma-Aldrich) dropwise under nitrogen. The addition of the reducing agent was continued dropwise until no more gas was evolved. The polymer-coated gold nanoparticles were then separated from "free" PEO-SH by membrane filtration (MWCO 30 000 Da, Millipore, Inc.) using dimethylformamide (DMF) as solvent. Finally, the PEO-coated gold nanoparticles (Au-PEO) were redispersed in methanol and washed by membrane filtration three times.

Thin Film Preparation. Solutions of the PSt-*b*-PMMA block copolymer (1 wt %) were prepared in benzene with various amounts of the Au-PEO nanoparticles added (from 0 to 10 wt % relative to block copolymer). Solutions were then spin-coated onto silicon substrates, and the film thickness was maintained at ∼40 nm for all samples. These films were annealed under saturated benzene vapor under the controlled humidity condition. The whole annealing process was performed in a home-built glovebox chamber at room temperature, as described elsewhere.[25]

The whole glovebox chamber was continually flushed with humid air, which was generated by bubbling air through warm water (∼50 °C). The relative humidity in the chamber was controlled by admixing dry air or adjusting the water temperature. Once the desired humidity condition was reached (∼90% in this work unless otherwise specified), it was maintained constant throughout the whole process. Inside the glovebox chamber, there is the much

* Authors for correspondence. E-mail: edkramer@mrl.ucsb.edu, joona@korea.ac.kr, and jeongsha@korea.ac.kr.
† Korea University.
‡ Materials Research Laboratory, UCSB.
§ Department of Materials, UCSB.
⊥ Department of Chemical Engineering, UCSB.
Department of Chemistry and Biochemistry, UCSB.

10.1021/ma071442z CCC: $37.00
Published on Web 10/04/2007

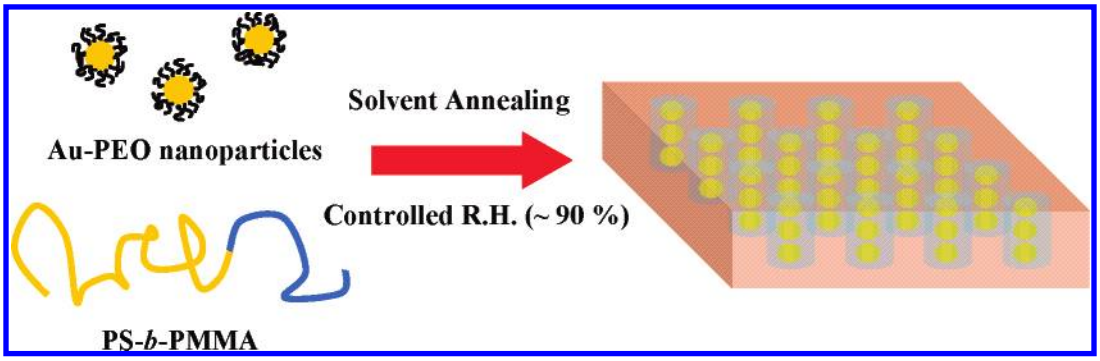

Figure 1. Graphical representation of the blending approach to the preparation of Au-PEO nanoparticle−PSt-*b*-PMMA hybrid thin films after solvent annealing under controlled humidity conditions.

smaller sealed inner chamber, an upside-down glass container on an larger glass Petri dish, under saturated benzene vapor where the relative humidity is initially the same as in the much larger outer chamber. The films were annealed for at least 12 h, and then the upside-down glass container was simply removed from the Petri dish inside the much larger glovebox, thus allowing the benzene in the swollen films to evaporate under a given humidity condition.

Characterization. After solvent annealing, the surface morphologies of thin films were characterized by scanning force microscopy (SFM) in noncontact mode. The SFM employed an etched n-type Si tip on a cantilever (ACTA, Applied NanoStructures) with a resonance frequency of 300 kHz and spring constant ranging from 25 to 75 N/m. The backside of the cantilever was coated with 30 nm thick Al. SEM images of the films were taken after UV irradiation, followed by a treatment with acetic acid and deionized water. The films were then coated with platinum by using ion sputtering, and the SEM was operated at 15 keV (Hitachi S-4300). For the TEM measurements, thin films were separated from the silicon oxide substrates by using 6:1 buffered oxide etchant (J.T. Baker). The films were floated on deionized water and transferred to carbon-coated copper mesh grids for TEM. The images were then obtained using a FEI Tecnai G2 microscope operating at 200 keV without staining.

Weight fractions of the Au core and PEO ligands were measured by thermal gravimetric analysis (TGA). Using the density of PEO (~1.2 g/cm^3) and the density of the Au core (~19.3 g/cm^3), the weight fractions of Au-PEO particles were converted into volume fractions. Au-PEO nanoparticle weight fractions of 1, 3, 5, 7, and 10 wt % correspond to Au-PEO nanoparticle volume fractions of 0.6, 1.9, 3.2, 4.5, and 6.5 vol %, respectively.

Results and Discussion

In examining the performance of PSt-*b*-PMMA block copolymers as templates for lithographic applications, a significant challenge is the long-range lateral ordering of the system and the requirement for a random copolymer neutralization layer. To overcome these challenges, it has recently been demonstrated that diblock/triblock copolymer films based on poly(styrene-*b*-ethylene oxide) (PSt-*b*-PEO) and poly(styrene-*b*-methyl methacrylate-*b*-ethylene oxide) (PSt-*b*-PMMA-*b*-PEO) exhibited cylindrical microdomains with a high degree of lateral ordering after solvent annealing under controlled humidity conditions.[26−28] In these examples, no neutralization layer is required, and it is believed that the relative humidity plays an important role in a lateral ordering of the block copolymer thin films, presumably by a strong interaction between the water vapor and the hydrophilic PEO domains during the solvent annealing process.[26] While such a process does not work directly with PSt-*b*-PMMA block copolymers, it is an intriguing possibility if a similar lateral ordering and vertical orientation can be induced in these hydrophobic systems by simple introduction of "external" hydrophilic moieties into PSt-*b*-PMMA copolymers.

In selecting an "external" hydrophilic moiety, PEO-coated gold nanoparticles (Au-PEO) were initially chosen because the Au-PEO nanoparticle diameter can be readily tuned in the sub-10 nm range, which allows these Au-PEO particles to be integrated into the block copolymer microdomains. Additionally, the inorganic Au core allows facile determination of the location of the nanoparticles by TEM.[11−14] Poly(ethylene oxide)-coated Au nanoparticles were therefore incorporated into poly(styrene-*b*-methyl methacrylate) (PSt-*b*-PMMA) diblock copolymers exhibiting a morphology consisting of cylindrical microdomains of PMMA in PSt. In this case, the PEO chains in Au-PEO are miscible with PMMA block in PSt-*b*-PMMA and have a strong repulsive interaction with the PSt block. Therefore, the Au-PEO nanoparticle should be selectively positioned within the PMMA domain if the particle size of Au-PEO is in the appropriate range. Figure 1 illustrates graphically the facile mixing process for formation of hybrid organic−inorganic thin films where the volume fractions of Au-PEO nanoparticles with respect to PSt-*b*-PMMA can be easily controlled and varied from 0.6 to 6.5%. To exclude any effect of film thickness on the ordering, the film thickness was kept constant at ~40 nm for all samples examined in this study. The resulting films were annealed under a saturated benzene vapor with controlled humidity (~90%) in an effort to obtain an overall cylindrical morphology which is not affected by addition of the Au-PEO nanoparticles.

The Au-PEO nanoparticles synthesized had a Au core diameter of 4.0 ± 1.0 nm and an overall diameter of 10.7 ± 2.5 nm and were mixed with PSt-*b*-PMMA diblock copolymers having an overall molecular weight of 140 kg/mol. On initial spin-casting it was found that the majority of Au-PEO nanoparticles were selectively positioned within the PMMA domains. The thin film morphology was investigated in detail after solvent annealing under controlled humidity (~90%). Parts a and b of Figure 2 represent the SFM images of surface structures when the volume fraction of Au−PEO is 0% and 4.5%, respectively. It can be seen that the effect of Au-PEO nanoparticles on the morphology of the PSt-*b*-PMMA films is significant. Without the Au-PEO nanoparticles, cylindrical microdomains are aligned parallel to the substrate, while perpendicular orientation of the same microdomains was achieved when 4.5 vol % of Au-PEO nanoparticles were incorporated. Note that black dots are observed within the bright PMMA domains in Figures 2b. A higher magnification SFM image (Figure 2c) shows these "dots" more clearly. Previously, it was demonstrated that the PEO microdomains at the free surface appear as depressed dimples in PEO-based block copolymer thin films,[25] due to the loss of water that swelled the PEO under the high humidity conditions that prevail during solvent evaporation. We therefore believe

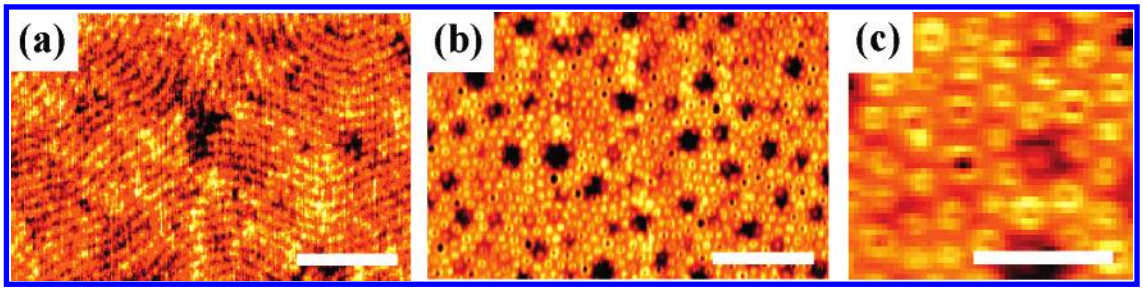

Figure 2. SFM height images taken from the PSt-*b*-PMMA thin films containing (a) 0 and (b) 4.5 vol % Au-PEO particles after solvent annealing and rapid solvent evaporation under high humidity conditions (~90%). (c) is a high-magnification SFM image of (b) showing "black dot" depressions at the surface of the PMMA cylinder domains.

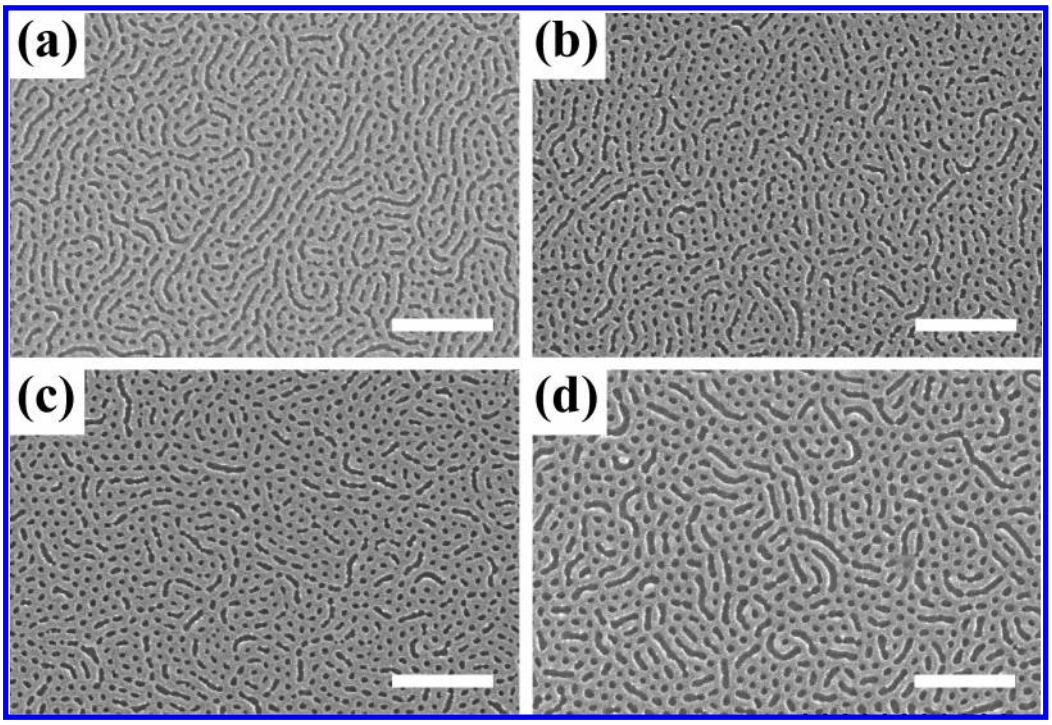

Figure 3. SEM images (top view) for PSt-*b*-PMMA thin films containing (a) 0, (b) 1.9, (c) 3.2, and (d) 4.5 vol % Au-PEO particles after solvent annealing and rapid solvent evaporation under low humidity conditions (~50%), followed by UV irradiation and then rinsing with acetic acid and water to remove the PMMA microdomains. Scale bar is 500 nm.

that the black dot features within the PMMA domains are due to hydrophilic Au-PEO nanoparticles. The larger features on the thin film surface are agglomerated Au-PEO nanoparticles at the surface which can be easily removed by washing with water.

Regarding the effect of humidity on the morphology, it should be noted that the Au-PEO nanoparticles play the same role as PEO blocks in PSt-*b*-PEO and PSt-*b*-PMMA-*b*-PEO block copolymers.[25−28] For example, when the films containing Au-PEO nanoparticles (from 0 to 4.5 vol %) were annealed under lower humidity conditions (~50%), the cylindrical microdomains are very poorly ordered and in many regions were oriented parallel to the substrate as seen in the SEM micrographs of films where the PMMA block has been degraded and removed as seen in Figure 3. Also significantly in SFM height images (not shown) of the surfaces of such samples before PMMA removal, no black dot features like those in the films produced under high humidity conditions are observed. This observation supports the hypothesis that the Au-PEO particles do not segregate significantly to the surface under low humidity conditions, an expected result since the surface energy of PEO is significantly higher than that of PMMA or PS.[30] This fact suggests that the ordering is induced by the interaction between water vapor and the hydrophilic Au-PEO nanoparticles, and the ordering mechanism is same as in the case of PEO-based block copolymers. During the solvent annealing step, the films are initially swollen with benzene under the saturated benzene atmosphere. Once the films were removed from the inner chamber, the solvent (benzene) in the films will evaporate from the top surface. Therefore, the surface becomes cooled and hence reaches the dew point. Under the high humidity condition within the glovebox chamber, the water vapor can condense on the cold surface and interact with the hydrophilic Au-PEO nanoparticles within the PMMA domains. As a consequence, the interaction between water and Au-PEO nanoparticles leads to the hexagonal arrays on the film surface. As the solvent evaporates further, the PMMA domains containing Au-PEO nanoparticles grow vertically and induce the perpendicular orientation of cylindrical microdomains. However, under the low humidity condition, the dew point will decrease so that water does not condense. As a result, the parallel orientation of cylindrical microdomains is observed at low humidity, as shown in Figure 3.

To fully investigate the morphology and structure of these nanocomposites that were prepared by solvent annealing under high humidity condition (~90%), the PMMA domains were removed by UV irradiation, followed by rinsing with acetic acid and water and SEM images were collected for films in which

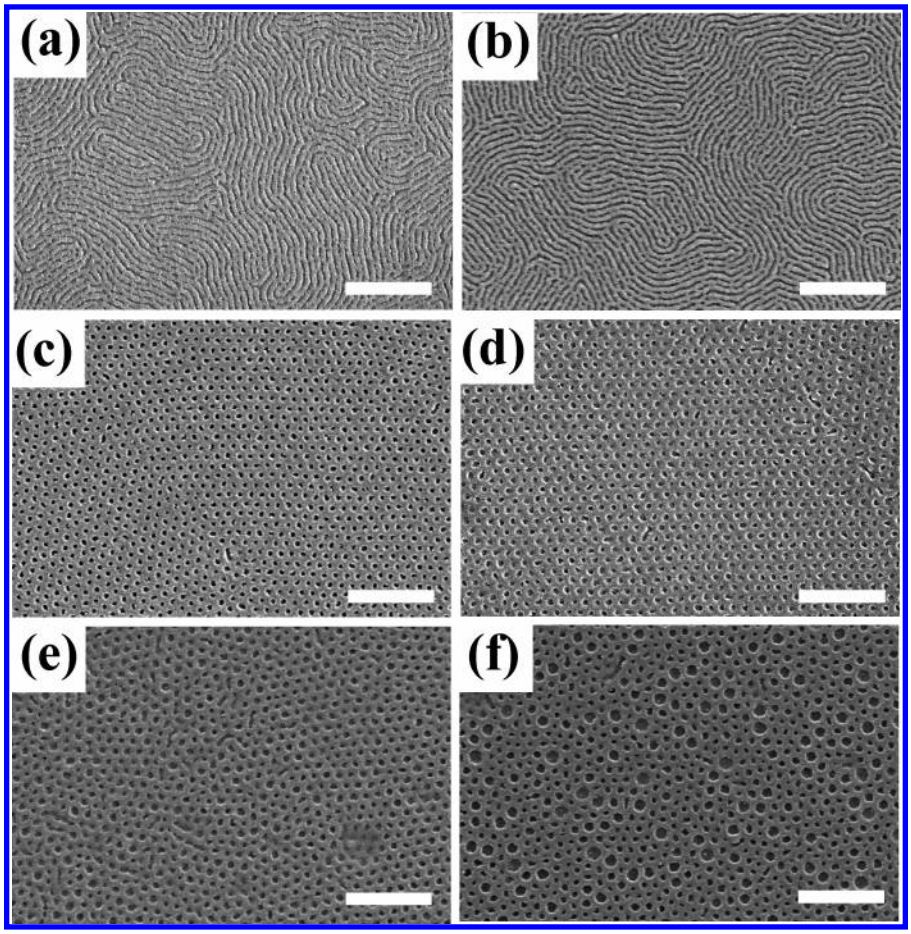

Figure 4. SEM images (top view) for PSt-*b*-PMMA thin films containing (a) 0, (b) 0.6, (c) 1.9, (d) 3.2, (e) 4.5, and (f) 6.5 vol % Au-PEO particles after solvent annealing and rapid solvent evaporation under high humidity conditions (~90%), followed by UV irradiation and then rinsing with acetic acid and water to remove the PMMA microdomains. Scale bar is 500 nm.

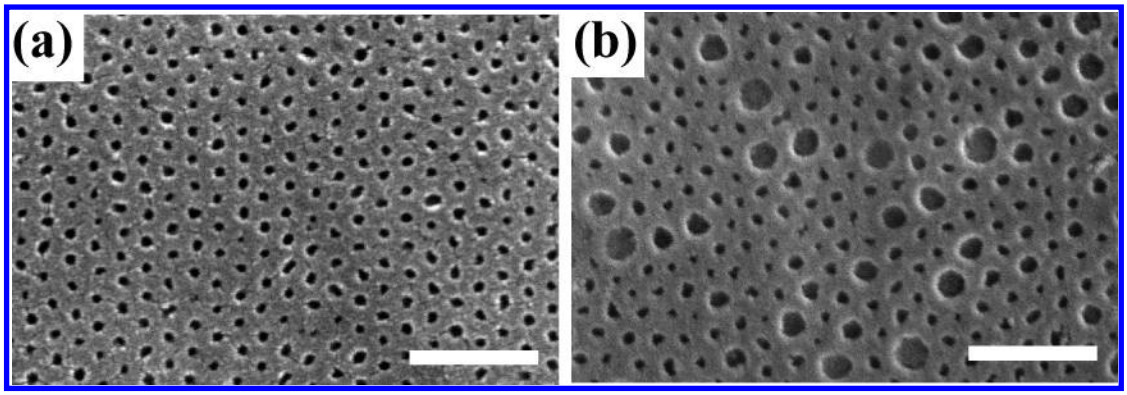

Figure 5. SEM images (bottom view) for PSt-*b*-PMMA thin films containing (a) 1.9 and (b) 6.5 vol % Au-PEO particles after solvent annealing and rapid solvent evaporation under high humidity conditions (~90%), followed by UV irradiation and then rinsing with acetic acid and water. Scale bar is 300 nm.

the volume fractions of Au-PEO nanoparticles were 0, 0.6, 1.9, 3.2, 4.5, and 6.5 vol % (Figure 4a−f). As expected, in the absence of Au-PEO nanoparticles, the film shows an orientation of cylindrical microdomains parallel to the substrate (Figure 4a) which is consistent with the SFM image in Figure 2a. This parallel orientation persists when 0.6 vol % of Au-PEO nanoparticles was added, but as the volume fraction of Au-PEO nanoparticle increases to 1.9%, the film morphology changes dramatically. At 1.9 and 3.2 vol %, it is evident that an orientation of cylindrical microdomains perpendicular to the film is achieved with pore diameter in Figure 4c,d of 24.2 ± 2.5 nm and periodicity of 67.2 ± 2.5 nm. Remarkably, it should also be noted that lateral ordering spans an area larger than 1 × 1 μm, which is significantly larger than the typical grain size, 200−300 nm, for PSt-*b*-PMMA block copolymers oriented by thermal annealing on a random copolymer brush.[18,19,31−33] This improved lateral ordering can be attributed to the effect of Au-PEO nanoparticles rather than to an intrinsic property of PSt-*b*-PMMA. Under the controlled high humidity condition (~90%), hydrophilic Au-PEO particles in the PMMA domains induce the lateral ordering as well as the perpendicular orientation, which is similar to what is observed for PEO-containing block copolymers. Further increasing the amount of Au-PEO nanoparticles to 4.5 and 6.5 vol %, leads to disruption of lateral ordering. At 4.5 vol % of Au-PEO, the pore size distribution becomes broader, ranging from 22 to 45 nm (Figure 4e), and

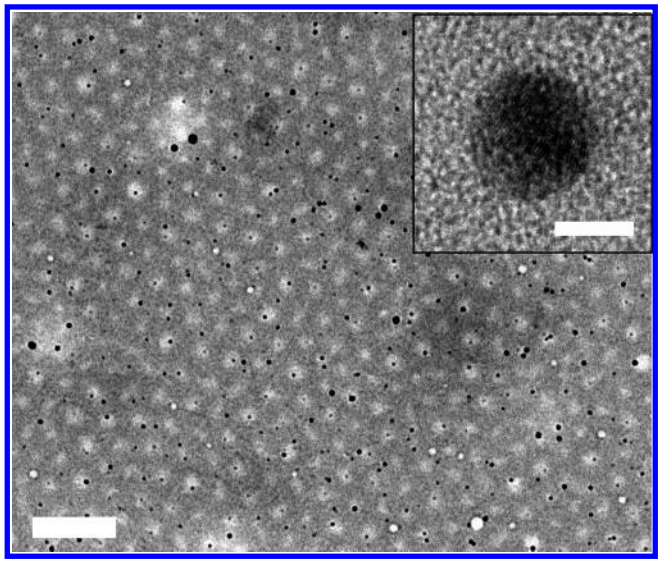

Figure 6. TEM images (top view) for PSt-*b*-PMMA thin film containing 4.5 vol % Au-PEO particles after solvent annealing and rapid solvent evaporation under high humidity conditions (~90%). Bright circles correspond to the PMMA microdomains and dark spots are gold nanoparticles. The inset is a high-magnification image of the core of a gold nanoparticle. Scale bars are 200 and 5 nm in the main image and the inset, respectively.

as a consequence, the hexagonal packing of the cylinders becomes distorted, while the cylindrical microdomains still orient perpendicularly. The pore size distribution is much broader, 25−60 nm in diameter, when 6.5 vol % of Au-PEO nanoparticles was added (Figure 4f), and this irregular pore size may be due to an inherent limitation in the amount of nanoparticles that can be blended into the block copolymer without disturbing its morphology. From the larger pore size and breadth of its distribution at 6.5 vol % Au-PEO, it seems likely that macrophase separation may be induced by large additions of Au-PEO nanoparticles in a similar way that large additions of PMMA homopolymers to PSt-*b*-PMMA diblock copolymer thin films leads to macrophase separation after thermal annealing.[34]

To examine whether the cylindrical microdomains persisted throughout the entire thickness of the block copolymer film, morphologies at the substrate interface were also examined. The substrate was removed by treatment with HF solution, and the liberated film was floated on surface of the HF solution and then flipped using another substrate. Parts a and b of Figure 5 are SEM images of the bottom of the films shown in parts c and f of Figure 4, respectively. Significantly, the structures at the top and bottom of these films are essentially the same once the PMMA and Au-PEO particles are removed, confirming that the perpendicular orientation of cylindrical microdomains persists throughout the whole thickness of the block copolymer film and therefore that these films can function as templates for lithographic applications.

The distribution of Au-PEO nanoparticles in the PSt-*b*-PMMA films was then investigated by TEM. Figure 6 is a top view, unstained TEM image for a film containing 4.5 vol % Au-PEO nanoparticles. The brighter areas correspond to the PMMA domains, whereas the PS matrix is shown as a darker background and the Au-PEO nanoparticles can be identified as dark spots. A high-resolution image of a Au core is shown in the inset. In Figure 6, it is evident that the majority of Au-PEO nanoparticles reside within the PMMA domains, which is consistent with the theoretical prediction by Balazs and co-workers.[5−7] In this system, the d/L ratio is ~0.4, which is estimated from the overall diameter of Au-PEO nanoparticles and the size of the PMMA domains. Therefore, one can expect that the Au-PEO nanoparticles should be localized at the center of PMMA domains. However, Figure 6 reveals that the particles are randomly dispersed within the PMMA domains, regardless of particle size. It is believed that this is due to the Au-PEO nanoparticles being "kinetically trapped" during the solvent annealing process and does not reflect the true equilibrium structure for this system. This can be compared with the recent study on the self-assembly of PS-coated gold nanoparticles within PSt-*b*-P2VP diblock copolymers.[11−14] In that case, near equilibrium morphologies could be obtained by slow evaporation of a neutral solvent. In contrast, the ordering of thin films in the system described above was achieved by fast evaporation of solvent under a high humidity condition.[25−28] Because of the miscibility between PEO chains and PMMA domains, the Au-PEO nanoparticles mostly reside within the PMMA domains, and they can interact with the water vapor at the surface to induce the ordering of thin films. However, the fast solvent evaporation does not allow the Au-PEO nanoparticles to achieve equilibrium localization at the center of the PMMA domains.

To highlight the significance of the solvent evaporation rate in the solvent annealing process, we also investigated the morphologies of films after solvent annealing where the benzene solvent was allowed to evaporate very slowly via a controlled leak from the inner chamber over about 24 h while a high humidity condition (~90%) was maintained. Figure 7 shows the resulting SEM images for films containing 1.9 and 3.2 vol % Au-PEO nanoparticles after the PMMA domains were removed. Compared to the morphologies of the same film compositions, Figure 4c,d, where such ordering was achieved by fast evaporation of solvent, it is evident that the slow

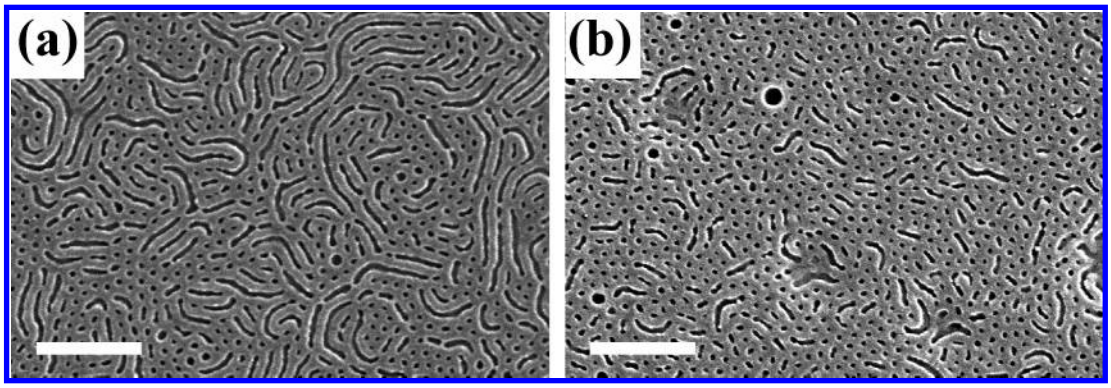

Figure 7. SEM images (top view) for PSt-*b*-PMMA thin films containing (a) 1.9 and (b) 3.2 vol % Au-PEO particles after solvent annealing and very slow solvent evaporation under high humidity conditions (~90%), followed by UV irradiation and then rinsing with acetic acid and water to remove the PMMA microdomains. Scale bar is 500 nm.

evaporation of solvent under high humidity conditions does not induce perpendicular orientation of cylindrical microdomains. Very poor ordering and mixed cylinder domain orientation results instead. The slow benzene evaporation produces negligible cooling of the film surface and thus no water vapor condensation.

The last aspect to consider is where in the thickness of film the Au-PEO nanoparticles are. As discussed above, the ordering in the thin films is induced by the Au-PEO nanoparticles interacting with the water vapor during the solvent annealing process. Therefore, it can be anticipated that a significant number of Au-PEO nanoparticles are segregated to the top surface of the film, where water vapor is condensed. As a result, black dots are clearly seen within the PMMA domains (Figure 2b,c), which is a strong indication of the presence of Au-PEO nanoparticles on the film surface. X-ray photoelectron spectroscopy results (not shown) confirm the presence of PEO as well as gold cores near the top surface of the film. Finally, these Au-PEO nanoparticles are completely miscible with water, and hence they can be easily washed away after PMMA degradation, followed by rinsing with acetic acid and water. Therefore, the resulting nanoporous templates can be used as a lithographic mask without spoiling the pattern transfer process due to the residual Au-PEO nanoparticles.

Conclusion

The blending of hydrophilic Au-PEO nanoparticles with thin films of PSt-*b*-PMMA block copolymers has been shown to induce the orientation of PMMA cylindrical microdomains perpendicular to the surface, which is in direct contrast to the parallel orientation observed when the nanoparticles are absent. As found for PEO-based block copolymer thin films, the key controlling factor is the solvent annealing process where the hydrophilic nanoparticles in PMMA domains interact with water vapor under the high humidity, solvent-swollen processing conditions. This strategy provides a simple route for the fabrication of ordered block copolymer templates from PSt-*b*-PMMA block copolymers without the need for a random copolymer neutralization layer while also allowing hybrid organic−inorganic materials with hierarchical order to be prepared. This adds a further degree of functionality to this important class of nanostructured materials.

Acknowledgment. This work was supported by the Korean Science and Engineering Foundation (KOSEF) grant funded by the Korea government (MOST) (No. ROA-2007-000-20102-0, M105030001 87-05M0300-18710), the Korea Research Foundation (Grant No. KRF-2004-005-C00068), and the UCSB Materials Research Lab. (NSF-DMR-MRSEC 05-20415). E.J.K. acknowledges support of the NSF Polymers Program (NSF-DMR 0704539).

References and Notes

(1) Hawker, C. J.; Russell, T. P. *MRS Bull.* **2005**, *30*, 952.
(2) Segalman, R. A. *Mater. Sci. Eng., R* **2005**, *R48*, 191.
(3) Balazs, A. C.; Emrick, T.; Russell, T. P. *Science* **2006**, *314*, 1107.
(4) Park, M.; Harrison, C.; Chaikin, P. M.; Register, R. A.; Adamson, D. H. *Science* **1997**, *276*, 1401.
(5) Thompson, R. B.; Ginzburg, V. V.; Matsen, M. W.; Balazs, A. C. *Science* **2001**, *292*, 2469.
(6) Thompson, R. B.; Ginzburg, V. V.; Matsen, M. W.; Balazs, A. C. *Macromolecules* **2002**, *35*, 1060.
(7) Lee, J. Y.; Thompson, R. B.; Jasnow, D.; Balazs, A. C. *Faraday Discuss.* **2003**, *123*, 121.
(8) Bockstaller, M. R.; Lapetnikov, Y.; Margel, S.; Thomas, E. L. *J. Am. Chem. Soc.* **2003**, *125*, 5276.
(9) Bockstaller, M. R.; Mickiewicz, R. A.; Thomas, E. L. *Adv. Mater.* **2005**, *17*, 1331.
(10) Spontak, R. J.; Shankar, R.; Bowman, M. K.; Krishnan, A. S.; Hamersky, M. W.; Samseth, J.; Bockstaller, M. R.; Rasmussen, K. *Nano Lett.* **2006**, *6*, 2115.
(11) Chiu, J. J.; Kim, B. J.; Kramer, E. J.; Pine, D. J. *J. Am. Chem. Soc.* **2005**, *127*, 5036.
(12) Kim, B. J.; Chiu, J. J.; Yi, G.-R.; Pine, D. J.; Kramer, E. J. *Adv. Mater.* **2005**, *17*, 2618.
(13) Kim, B. J.; Bang, J.; Hawker, C. J.; Kramer, E. J. *Macromolecules* **2006**, *39*, 4108.
(14) Kim, B. J.; Given-Beck, S.; Bang, J.; Hawker, C. J.; Kramer, E. J. *Macromolecules* **2007**, *40*, 1796.
(15) Lin, Y.; Boeker, A.; He, J.; Sill, K.; Xiang, H.; Abetz, C.; Li, X.; Wang, J.; Emrick, T.; Long, S.; Wang, Q.; Balazs, A.; Russell, T. P. *Nature (London)* **2005**, *434*, 55.
(16) Kim, B. J.; Fredrickson, G. H.; Hawker, C. J.; Kramer, E. J. *Langmuir* **2007**, *23*, 7804.
(17) Mansky, P.; Liu, Y.; Huang, E.; Russell, T. P.; Hawker, C. J. *Science* **1997**, *275*, 1458.
(18) Huang, E.; Pruzinsky, S.; Russell, T. P.; Mays, J.; Hawker, C. J. *Macromolecules* **1999**, *32*, 5299.
(19) Ryu, D. Y.; Shin, K.; Drockenmuller, E.; Hawker, C. J.; Russell, T. P. *Science* **2005**, *308*, 236.
(20) Drockenmuller, E.; Li, L. Y. T.; Ryu, D. Y.; Harth, E.; Russell, T. P.; Kim, H.-C.; Hawker, C. J. *J. Polym. Sci., Part A: Polym. Chem.* **2005**, *43*, 1028.
(21) Ludwigs, S.; Böker, A.; Voronov, A.; Rehse, N.; Magerle, R.; Krausch, G. *Nat. Mater.* **2003**, *2*, 744.
(22) Stoykovich, M. P.; Muller, M.; Kim, S. O.; Solak, H. H.; Edwards, E. W.; de Pablo, J. J.; Nealey, P. F. *Science* **2005**, *308*, 1442.
(23) Rzayev, J.; Hillmyer, M. A. *J. Am. Chem. Soc.* **2005**, *127*, 13373.
(24) Listak, J.; Bockstaller, M. R. *Macromolecules* **2006**, *39*, 5820.
(25) Bang, J.; Kim, B. J.; Stein, G. E.; Russell, T. P.; Li, X.; Wang, J.; Kramer, E. J.; Hawker, C. J. *Macromolecules* **2007**, *40*, 7019.
(26) Bang, J.; Kim, S. H.; Drockenmuller, E.; Misner, M. J.; Russell, T. P.; Hawker, C. J. *J. Am. Chem. Soc.* **2006**, *128*, 7622.
(27) Kim, S. H.; Misner, M. J.; Russell, T. P. *Adv. Mater.* **2004**, *16*, 2119.
(28) Kim, S. H.; Misner, M. J.; Xu, T.; Kimura, M.; Russell, T. P. *Adv. Mater.* **2004**, *16*, 226.
(29) Yee, C. K.; Jordan, R.; Ulman, A.; White, H.; King, A.; Rafailovich, M.; Sokolov, J. *Langmuir* **1999**, *15*, 3486.
(30) Wu, S. *Polymer Handbook*, 3rd ed.; Wiley: New York, 1989; p VI411.
(31) Kim, H.-C.; Jia, X.; Stafford, C. M.; Kim, D. H.; McCarthy, T. J.; Tuominen, M.; Hawker, C. J.; Russell, T. P. *Adv. Mater.* **2001**, *13*, 795.
(32) Mansky, P.; DeRouchey, J.; Russell, T. P.; Mays, J.; Pitsikalis, M.; Morkved, T.; Jaeger, H. *Macromolecules* **1998**, *31*, 4399.
(33) Thurn-Albrecht, T.; Schotter, J.; Kastle, G. A.; Emley, N.; Shibauchi, T.; Krusin-Elbaum, L.; Guarini, K.; Black, C. T.; Tuominen, M. T.; Russell, T. P. *Science* **2000**, *290*, 2126.
(34) Jeong, U.; Ryu, D. Y.; Kho, D. H.; Lee, D. H.; Kim, J. K.; Russell, T. P. *Macromolecules* **2003**, *36*, 3626.

MA071442Z